

Simulation of Membrane and Cell Culture Permeability and Transport

Michael B. Bolger and Viera Lukacova
Simulations Plus, Inc.

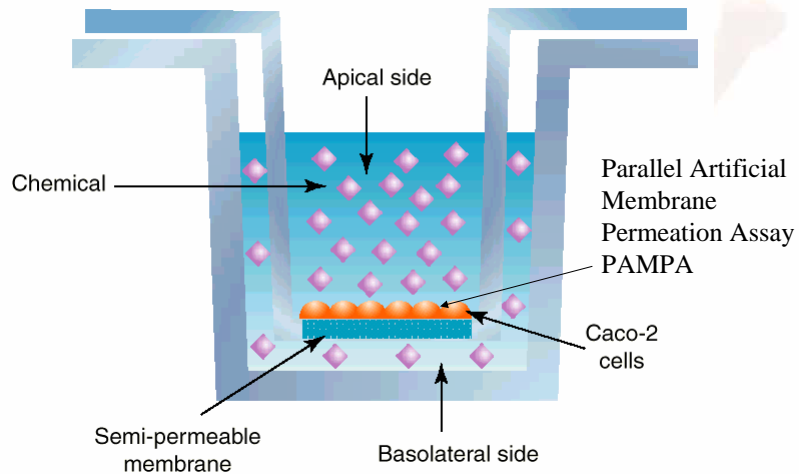
GPEN, Kansas, 2006

Outline

- Models of microscopic membrane kinetics
- Calculation of membrane entry and exit kinetics.
- Simulation of passive permeability
- Application to efflux transporter Pgp

GPEN, Kansas, 2006

Epithelial Cell Permeability Assay

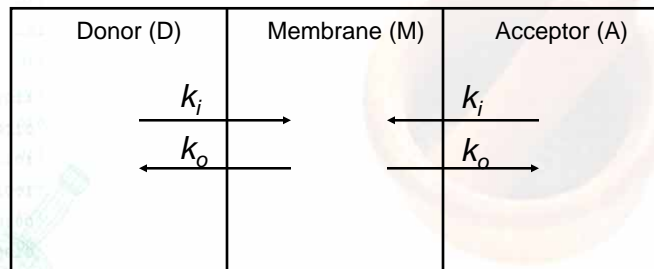


Li, A.P., DDT, 6(7):339-348

GPEN, Kansas, 2006

Simplest model

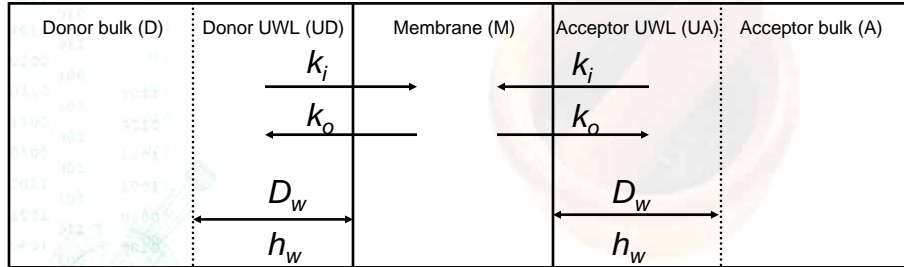
only the partitioning in and out of the membrane
 no concentration gradients
 the concentration equilibrium in each compartment reached instantaneously



GPEN, Kansas, 2006

Extended model 1

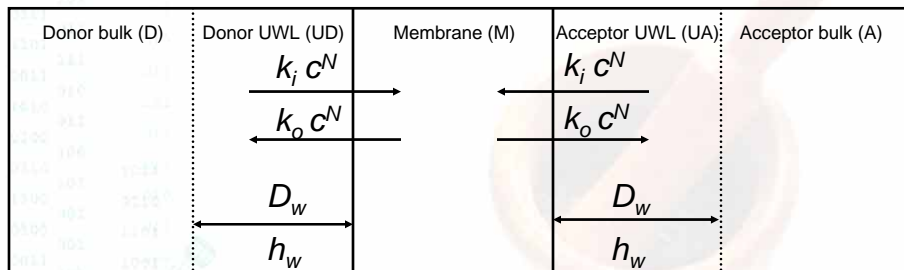
Addition of diffusion through unstirred water layer (UWL) in donor and acceptor compartments concentration equilibrium in bulk aqueous phases and membrane - instantaneous



GPEN, Kansas, 2006

Extended model 2 - model currently in use

Addition of ionization of compounds
Assume the diffusion through the aqueous phases is the same for neutral and ionized species partitioning into the membrane - only non-ionized species.



$$c_x^N = c_{Ux} \frac{1}{1 + \sum_{r=1}^j 10^{\sum_{s=r}^j pKa_s^b - (j-r+1) \times pH} + \sum_{p=1}^i 10^{p \times pH - \sum_{s=1}^p pKa_s^a}}$$

c_U - total concentration of the drug in the membrane vicinity
 c^N - concentration of un-ionized species
 a and b - acidic and basic pKa
 i and j - number of acidic and basic pKas
 x - acceptor or donor (pH in acceptor and donor compartments may be different)

GPEN, Kansas, 2006

Membrane Composition

- Kansy, M. et al., J. Med. Chem. 41(7):1007 (1998)
 - 1-20% phosphatidylcholine (PC) in hexadecane
- (BAMPA) (Sugano K., et al., Int. J. Pharmaceut. 228:181 (2001))
 - biomimetic lipid composition similar to intestinal brush border membrane.
 - PC (0.8%)
 - Phosphatidylethanolamine (PE, 0.8%)
 - Phosphatidylserine (PS, 0.2%)
 - Phosphatidylinositol (PI, 0.2%)
 - Cholesterol (CHO, 1.0%)
- Collander R. Acta. Chem. Scand., 5:774 (1951)
 - $\log P_{PC/water} = \log(\alpha) + \beta \log P_{octanol/water}$
 - with parameters: $\alpha=15$ and $\beta=0.73$ and $R^2 \approx 0.73$

GPEN, Kansas, 2006

Membrane Kinetics

Prediction of rate constants k_i and k_o for partitioning to and out of the membrane. Using the relationship and parameters ($\gamma=0.48$ and $\delta=0.286$) from Kubinyi:

$$k_i = \frac{\gamma P}{\delta P + 1}; \quad k_o = \frac{\gamma}{\delta P + 1}$$

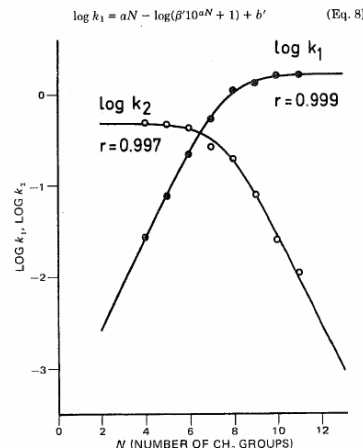
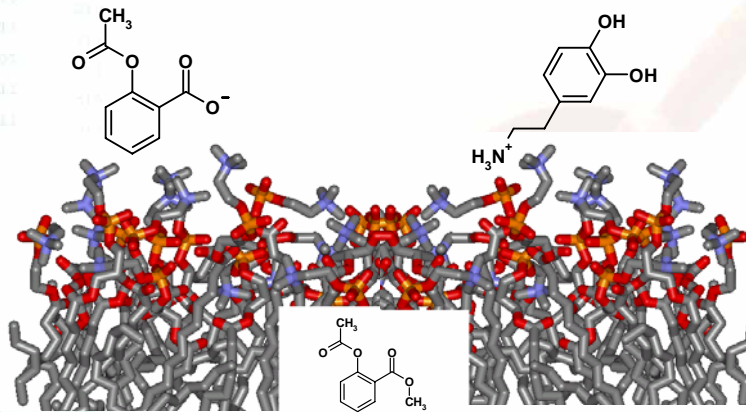


Figure 2—Rate constants k_1 and k_2 of the partitioning of homologous quaternary alkylammonium bromides; comparison of experimental values from a three-compartment system (sodium bromide added) (2) and values calculated from Eqs. 8 and 9 (a, b, β , and c values from Table I).

GPEN, Kansas, 2006

Kubinyi, H., J. Pharm. Sci. 67:262 (1978)

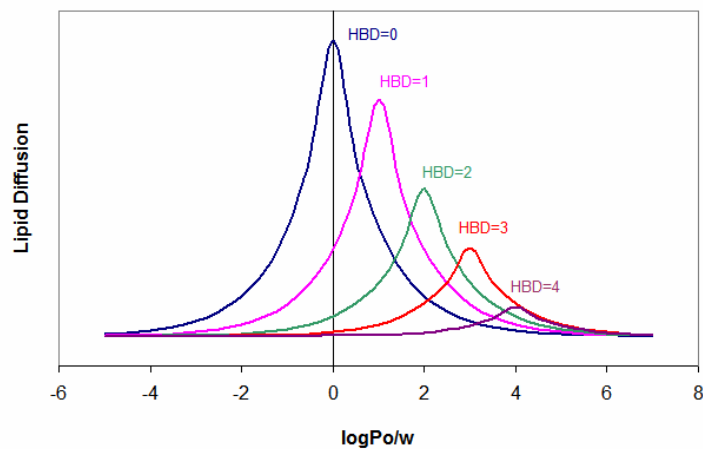
Passive Permeability Transcellular



f (Hydrophobicity, H-Bonding, Ionization)

GPEN, Kansas, 2006

Theoretical Lipid Diffusion as a function of log P and HBDs

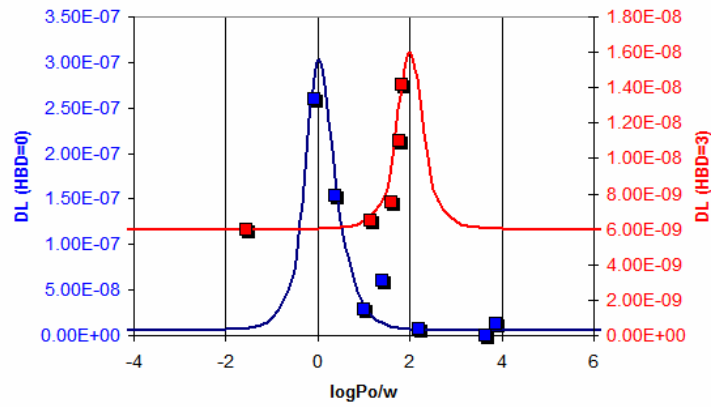


$$LD = LD_0 + LD_{\max} * \exp(-\text{abs}(\text{HBD} - \log P_o/w))$$

GPEN, Kansas, 2006

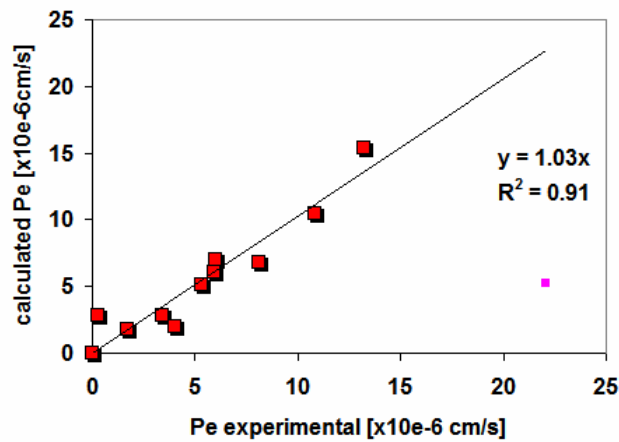
Optimized Lipid Diffusion

Optimized Lipid Diffusion for caffeine, antipyrine, flumazenil, coumarin, griseofulvin, clofibrate, progesterone, acyclovir, chloramphenicol, hydrocortisone, methylprednisolone



GPEN, Kansas, 2006

Pe calculated using DL modeled by theoretical relationship between DL and logPo/w for HBD=0 and HBD=3



GPEN, Kansas, 2006

Membrane Accumulation for high log P molecules.

Dvorsky-Balaz J. Theor. Biol.185:213 (1997)

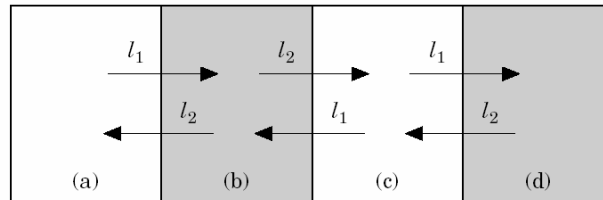


FIG. 1. The schematic outline of the system consisting of four alternating aqueous [white (a, c)] and lipid [grey (b, d)] phases. The lipid phases represent a membrane and either the hydrophobic core of a globular protein or further membrane. The transport rate is characterized by the rate parameters l , the subscripts indicating the direction of transport (1—from water to a lipid phase and 2 backwards).

GPEN, Kansas, 2006

Membrane Accumulation for high log P molecules.

Dvorsky-Balaz J. Theor. Biol.185:213 (1997)

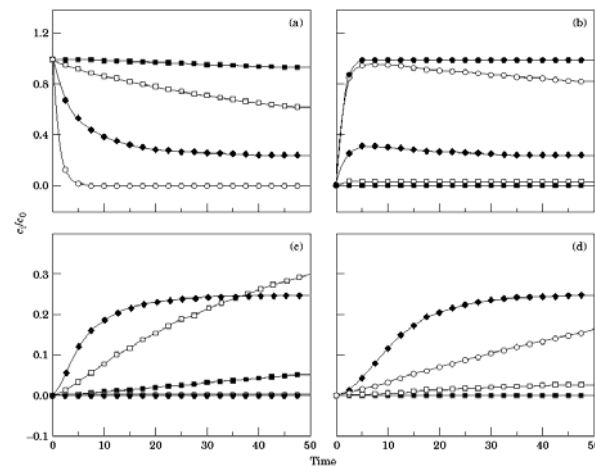
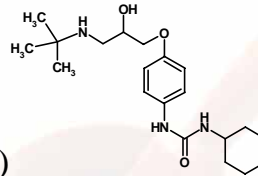


FIG. 2. The transport kinetics of the compounds differing in their partition coefficient P in individual compartments (Fig. 1) indicated by (a)–(d) in the corners of the insets. Calculated from eqn (3) using eqn (5) with the constants $\gamma = 0.245$ and $\delta = 0.286$ (Kubinyi, 1978). Individual curves hold for $\log P = -2$ (■), -1 (□), 0 (◆), 2 (◇), and 4 and more (●). In (a), the last two curves are overlaid, the first and the last curve are overlaid in (d).

GPEN, Kansas, 2006

Talinolol



- $\log D_{9.4} = 3.14$ (Langguth)
- Basic $pK_a = 9.8$ (QMPRPlus)
- Composite Pgp $K_m = 412 \mu\text{M}$ (149 $\mu\text{g/mL}$)
 - Two sites high (72 μM) and low (1570 μM) (Langguth)
- Solubility = 1.23 mg/mL (pH = 7.4) (Gramatte)
- $\text{Peff}_{\text{rat}} = 0.5 \times 10^{-4} \text{ cm/s}$ (Langguth)
- $\text{Peff}_{\text{QMPR}} = 1.68 \times 10^{-4} \text{ cm/s}$

GPEN, Kansas, 2006

Image J Analysis of Pgp Micropig

H. Tang, AAPS Annual meeting poster, 2002

RT-PCR
expression of
mRNA

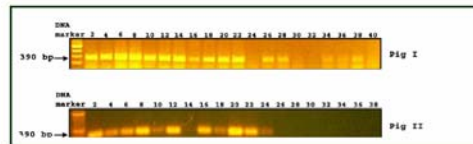
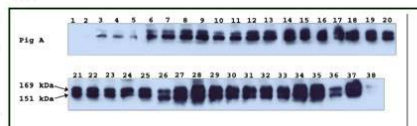
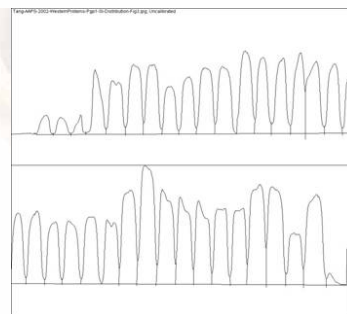


Fig 2. RT-PCR detection of *p-gp* 1 expression in two pigs. The even alternating numbers from 2 to 40 indicate segments from the proximal duodenum to the distal ileum.



Western blot of Pgp-1 from
proximal to distal SI



GPEN, Kansas, 2006

Mouly, S., Paine, M.F. PharmRes-20(10):1595-1598 (2003)

Pgp expression in human SI

P-gp Expression along the Human Small Intestine

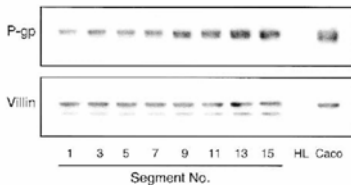


Fig. 1. Western blot showing the expression of P-glycoprotein and the control protein villin along the length of a human donor small intestine (HI-31). Segment 1 represents duodenum; segments 3, 5, and 7 represent middle to distal jejunum; and the remaining segments represent ileum. All segments measured approximately 30 cm in length. For a given intestine, the same blot was probed for both proteins, but optimal visualization of each required a different exposure time. HL, human liver homogenate. Caco, homogenate prepared from a representative Caco-2 cell monolayer treated with the CYP3A4/P-gp inducing agent 1 α ,25-(OH) $_2$ -D $_3$. All lanes of the gel were loaded with 15 μ g homogenate protein.

Table II. Relative P-gp Expression* Along the Length of Four Human Donor Small Intestines

Segment [†]	Donor code [‡]			
	HI-31	HI-32	HI-35	HI-40
Duodenum/proximal jejunum				
1/2	0.51	0.63	0.33	0.68
Middle to distal jejunum				
3/4	0.61	0.61	0.51	0.85
5/6	0.61	0.81	0.50	0.99
7/8	0.70	0.72	0.57	0.88
Ileum				
9/10	0.89	0.72	0.50	0.97
11/12	0.92	0.74	0.69	1.00
13/14	0.86	0.73	0.80	0.91
15/16	1.00	0.86	0.59	
17/18		1.00	1.00	
20		0.89		

* P-gp/villin IOD ratio (normalized to the maximum value).

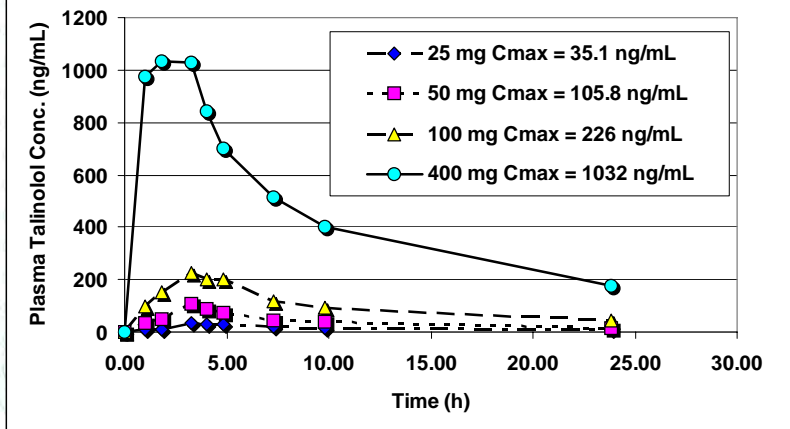
[†] Each segment measured approximately 30 cm in length.

[‡] HI, human intestine.

GPEN, Kansas, 2006

Talinolol Non-linear Dose Dependence

Talinolol Dose Dependence
de Mey et al. J. Cardio. Pharmacol. 26(6):879 (1995)



GPEN, Kansas, 2006

Regional Window for Absorption

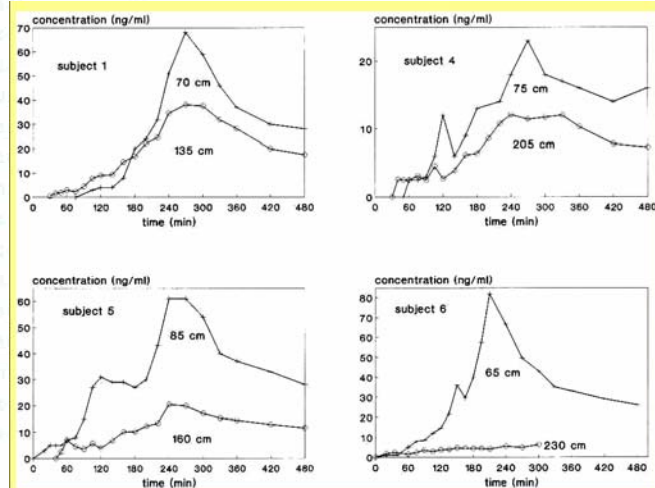
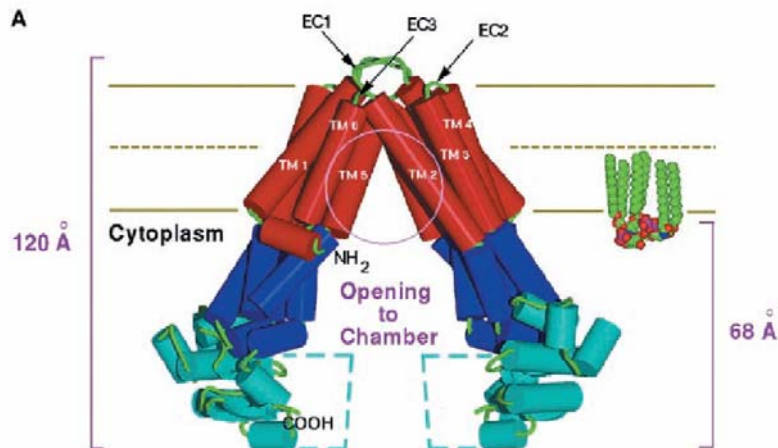


Fig. 3. Typical serum talinolol concentration-time profiles after a 160-minute perfusion of dissolved talinolol into different parts of the small intestine. Numbers under the curves correspond to the position of the perfusion site (in centimeters beyond the teeth). Note different scaling on the concentration axes.
From: Gramatte: Clin Pharmacol Ther, Volume 59(5), May 1996, 541-549

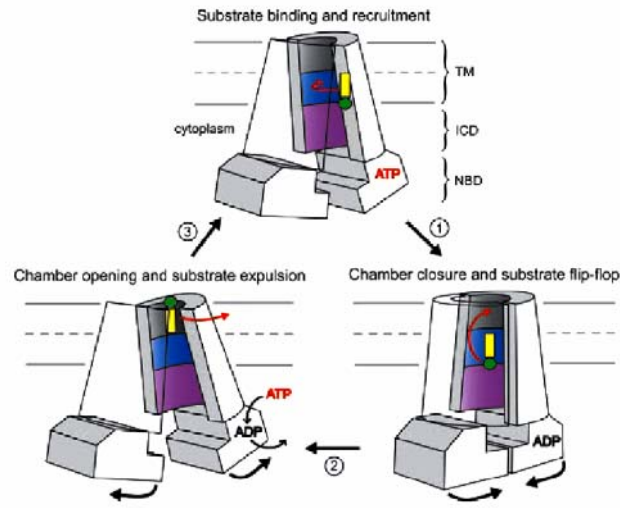
GPEN, Kansas, 2006

ATP-Binding Cassette Protein Msb (1JSQ) from E. Coli Chang, Science 293:1793 (2001)



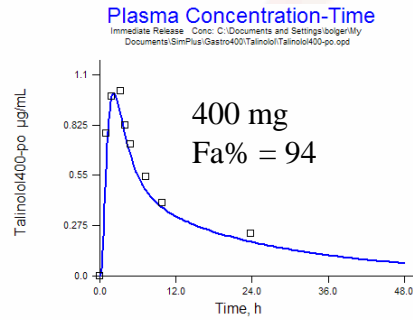
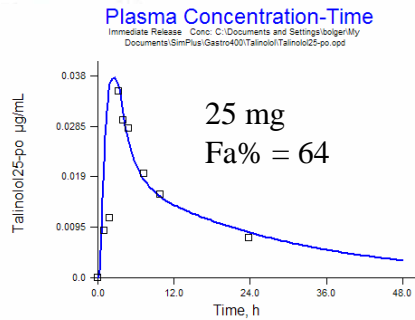
GPEN, Kansas, 2006

ATP-Binding Cassette Protein Msb (IJSQ) from E. Coli
 Chang, Science 293:1793 (2001)

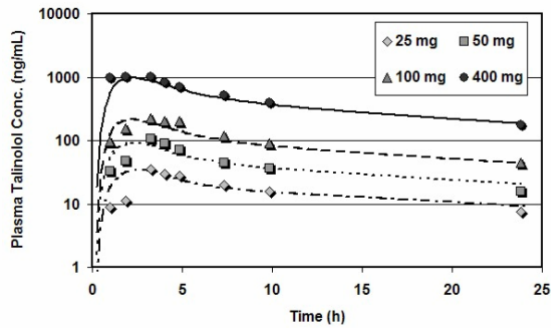


GPEN, Kansas, 2006

25 and 400 mg Talinolol *po*
 Data from: de Mey, C., J. Cardiovasc. Pharmacol. 26(6):879 (1995)
 courtesy of Peter Langguth and Daniel Wagner



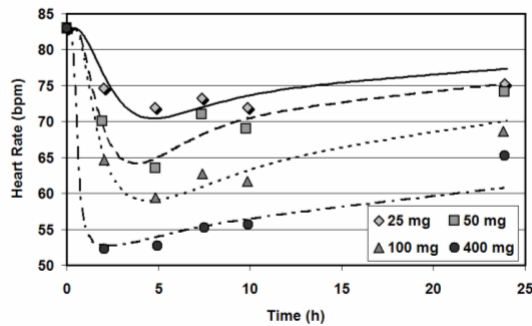
GPEN, Kansas, 2006



GastroPlus PK PD - Simulation of Talinolol Effect on Heart Rate

Tubic M, 2006 in press.

GPEN, Kansas, 2006



Conclusions

- Membrane and cellular simulations can improve our understanding of absorption.
- Membrane concentration is important for calibration of *in vitro* transporter kinetics.
- The present state-of-the-art provides useful (not perfect) simulations.

GPEN, Kansas, 2006